



Research Article

LOCAL-BEHAVIOR DETERMINATION FOR AN OMNIDIRECTIONAL MOBILE ROBOT USING AN INTEGRATION-TYPE SONAR RING

T. Emaru^{1,*}

H. Sato²

Y. Kobayashi¹

¹ Faculty of Engineering, Hokkaido University,
N13W8, Sapporo, Hokkaido
0608628, Japan

² Graduate school of Engineering, Hokkaido University,
N13W8, Sapporo, Hokkaido
0608628, Japan

ABSTRACT:

Time-of-flight ranging methods are generally utilized to measure distance using an ultrasonic wave sensor. However, faint reflected waves tend to be overlooked by this method. We have proposed an integration-type ultrasonic wave sensor that effectively uses faint reflected waves. This paper proposes a local-behavior determination method for autonomous mobile robots using a sonar ring, which consists of multiple integration-type ultrasonic wave sensors. This sonar ring can reduce the sensing time because it simultaneously obtains information from multiple directions. We apply our previously developed path-generation method to an omnidirectional mobile robot. Generally, the objective of a mobile robot is to reach a target position as quickly as possible. At the same time, the robot is required to avoid collisions with obstacles. Therefore, it needs to slow down to safely bypass obstacles in high-obstacle-density environments. This paper also proposes a method for controlling the velocity of the robot by generating the target acceleration. Our proposed method takes the upper limit of the input torque into account. Experimental results show that in the presence of obstacles in the vicinity of the mobile robot, the proposed method can decrease the velocity of the mobile robot in order to avoid collision with obstacles.

Keywords: *Ultrasonic wave sensor, Autonomous mobile robot, Obstacle avoidance*

1. INTRODUCTION

Recently, studies on autonomous robots have been conducted in various fields. Robots need to determine their actions on the basis of the surrounding environment, so a robot is required to perceive environmental information using its external sensors.

In this study, we propose a robust path-generation method, which utilizes ultrasonic sensors. Time-of-flight ranging methods are generally employed to measure distance with an ultrasonic sensor and are widely used for obstacle avoidance [1-2], localization [3], map construction [4-6], and so on. However, faint reflected waves are not usually detected by these methods. Therefore, we have proposed an integration-type ultrasonic wave sensor that effectively uses faint reflected waves [7-9]. Recently, SLAM (Simultaneously Localization And Mapping) [10] has been lively discussed in the field of mobile robot. In this research area, not only ultrasonic wave sensor, but also other sensors such as laser range finder, IMU sensor [11], camera, RGB-D (RGB Depth) sensor [12] and so on are often used.

* Corresponding author: T. Emaru
E-mail address: emaru@eng.hokudai.ac.jp



However, ultrasonic wave sensor has the following advantages: low cost, easy-to-implement, safe for the environment. Therefore, in this study, we propose a novel sensing technique which utilizes ultrasonic wave sensor. In our previous studies, we used a sonar that can be rotated by motors. The advantage of this method is that it has a simplified system configuration, but it takes a relatively longer time to obtain environmental information because it contains motor as a driving part. This paper proposes a local-behavior determination method for autonomous mobile robots that employs sonar ring, which consists of integration-type ultrasonic wave sensors. The proposed sonar ring can decrease the measurement time because it can simultaneously obtain information from multiple directions. To confirm the validity of the proposed system, we applied the path-generation method.

The paper is arranged as follows: Section 2 explains the system configuration of the integration-type ultrasonic sensor and sonar ring, which consists of several integration-type ultrasonic sensors. Section 3 describes the path-generation method, and Section 4 explains the method used for determining the target angular velocity and speed of the mobile robot. We conducted several experiments applying the proposed method. Sections 5 and 6 present the results and conclusions, respectively.

2. INTEGRATION-TYPE ULTRASONIC SENSOR

This section explains the measurement principle of an integration-type ultrasonic sensor, after which we explain the sonar-ring system.

2.1 Measurement principle of the proposed method

Figure 1 shows the system configuration of an integration-type ultrasonic sensor. An analog circuit is utilized to process the reflected sonar waves as follows:

1. Amplify the reflected wave using an instrument amplifier.
2. Obtain the absolute value by using an absolute-value circuit.
3. Perform integration and obtain the integration value; the integration value is then digitized by analog to digital conversion at a specific time.

The digitized integration value is brought in the range of 0-1023 with the use of a 10bit A/D converter.

2.2 System configuration of integration-type sonar ring

In this study, by assembling 16 integration-type ultrasonic sensors at 11.25 degree intervals, we produced a sonar ring with a radius of 19 cm, as shown in Fig. 2. In this research, we utilize a transducer whose opening angle is 40 degree. Therefore, in case of 20 degree intervals, we can obtain redundant data from two transducers. However, it is very difficult for ultrasonic wave sensor to receive reflected wave from slanted object. Therefore, in order to increase redundancy of the sensing system, we set the interval as above.

Figure 3 shows the system configuration of the integration-type sonar ring. Each sonar is controlled by a one-chip microcomputer, H8/3694, but it can control only four sets of sonars. Because 16 sets of sonars are required in the proposed system, we utilize four H8/3694 computers that are connected by an I²C-bus. Figure 4 shows the circuit board with a one-chip microcomputer and analog circuit for controlling the four sets of integration-type sonars. We utilized four sets of this circuit board to control 16 sets of integration-type sonars.

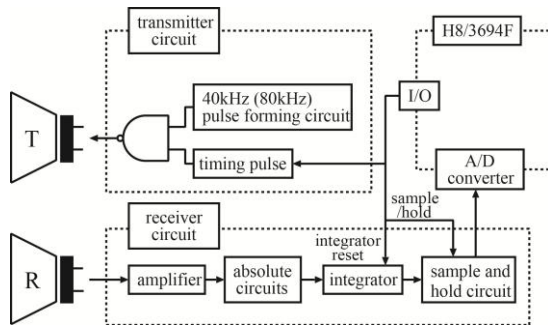


Fig. 1. System configuration of the integration-type ultrasonic sensor.

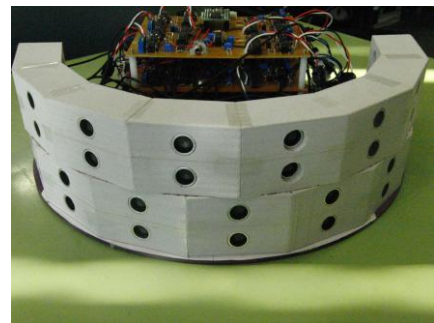


Fig. 2. Overview of the integration-type sonar ring.

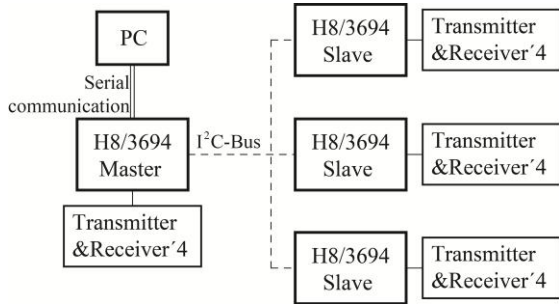


Fig. 3. System configuration of the proposed sonar ring.

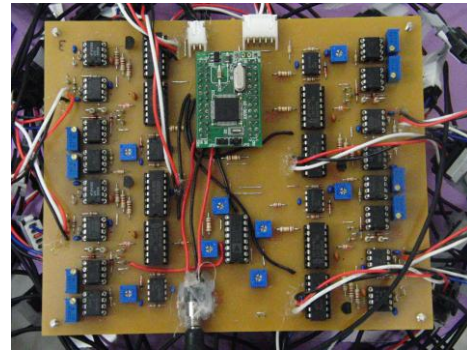


Fig. 4. Circuit board to control four sensors.

3. PATH GENERATION METHOD

The robot used in this study can avoid obstacles by generating a target angle and a target path based on the target angle. This section describes the method of generation of the target angle. The proposed sonar ring consists of 16 integration-type ultrasonic sensors. In this section, we explain the general method of generation of the target angle assuming that the sensors are positioned at equal intervals on the front side of the mobile robot.

We represent the angle of each sensor in the polar coordinate system, whose origin is the current position of the mobile robot, and consider its front direction to be 90 deg. Then, we number the sensors in order starting from the smallest angle subtended by it at the origin, and represent the angle corresponding to the i -th sensor as θ_i , as shown in Fig. 5. The target angle is represented in the same polar coordinate system as the angle of the sensors.

The target path is in the form of an arc, which is generated by the robot as it moves, when the robot determines the target angle, and the slope of whose tangent line at the point is θ_i . Although the difference between the target angle and the direction in which the robot moves increases continuously, the robot moves in nearly the same direction as the target angle because the target angle is generated within a short period.

The i -th sensor acquires the integration value $integration(i)$ and distance value $distance(i)$ for each sampling interval. By the way, upper limit of the speed of the robot is about 30 cm/s in our system. Therefore, we set sensing range of the sonar at 200 cm, and determined the sampling time by using it as a reference. The robot generates the target angle from these values as follows:

1. The threshold Thr_{int} to binarize the integration values is determined on the basis of these target values.
2. The robot binarizes $integration(i)$ using Thr_{int} and examines the passable area. The robot focuses on the area in which the integration values are smaller than Thr_{int} on the basis of the principle that the direction with a smaller integration value is safer. If multiple areas satisfy this condition, the broadest area of them is determined as M , and the center angle of M is determined as θ'_p .
3. Then, θ_p is determined as the smooth time-series data of θ'_p .
4. The moving speed v and angular velocity ω are determined. The next section explains the algorithm used to determine these parameters in detail.
5. Finally, an arc-like path is generated from θ_p , v and ω .

3.1 Determination of threshold

Figure 7 shows the integration value obtained in Fig. 6. In our previous studies, we utilized the mean of the integration values as the threshold Thr_{int} . However, it is very difficult to recognize obstacles using this threshold.

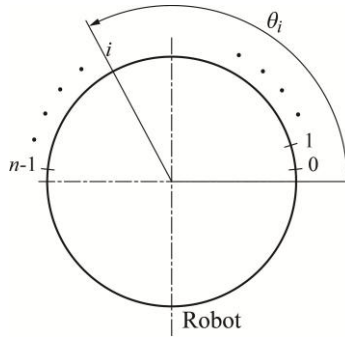


Fig. 5. Arrangement of sensors.

Therefore, we propose a new threshold that is smaller than the mean of the integration values. As shown in Fig. 7, the new threshold is formulated by the average of the minimum value of the obtained integration values and their means.

3.2 Deadlock avoidance

The proposed method enables the mobile robot to move in a relatively safer direction within the sensing range. Therefore, the robot may move toward the wall if there is no passable area within the sensing range. Then, we propose a method for detecting deadlocks. The robot rotates by 180 degrees when it determines that there is no passable area in its front.

The following data were used to determine the presence of a passable area.

- u_1 : Mean of the integration values
- u_2 : Minimum integration values in the area M , where M is an area that is smaller than the threshold.
- u_3 : Width of M

If multiple candidates of M exist, as shown in Fig. 7, the area with the maximum width is adopted as M . The parameters u_1 , u_2 , and u_3 are formulated as follows:

$$u_1 = \sum_{i=0}^{n-1} \text{integration}(i) / n \quad (1)$$

$$u_2 = \min_{\alpha_M \leq i \leq \beta_M} \{ \text{integration}(i) \} \quad (2)$$

$$u_3 = \beta_M - \alpha_M \quad (3)$$

Here α_M and β_M are the angles at both ends of M ($\alpha_M \leq \beta_M$). We multiply these values by w_i ($i=1,2,3$) respectively, and the difference between the sum of these values and a constant c is denoted by x given by Eq. (4).

$$x = \sum_{i=1}^3 w_i u_i - c \quad (4)$$

In another analogy, it is considered as a neural network. Namely u are inputs to the network, w are weights of the inputs, and c is threshold. Then, x is converted into ζ using the sigmoid function. Figure 8 shows the schematic diagram of the proposed method. We define ζ as follows:

$$\zeta(x) = 1 / (1 + e^{-x}) \quad (5)$$

Finally, the robot determines that there is no passable area within the sensing area when ζ surpasses the threshold.

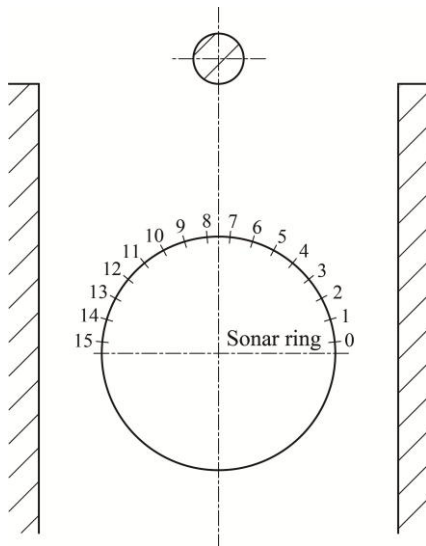


Fig. 6. Experimental environment 1.

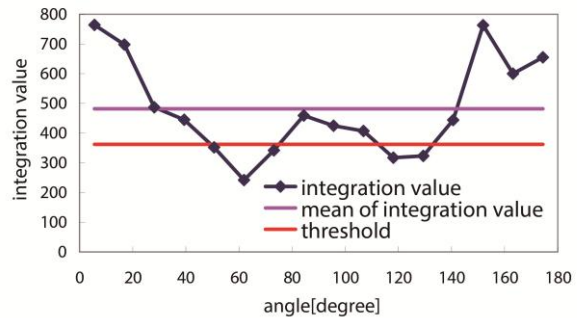


Fig. 7. Proposed threshold obtained in experimental environment 1.

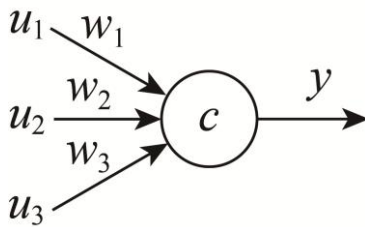


Fig. 8. Schematic diagram of passability determination.

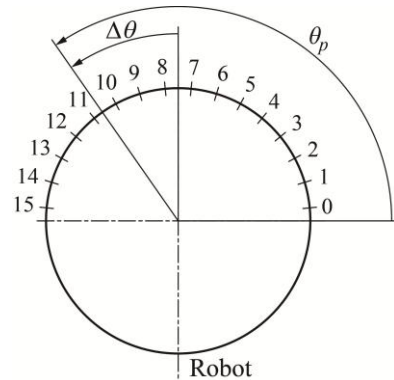


Fig. 9. Difference between the target angle and the forward direction of the robot.

4. DETERMINATION OF TARGET VALUE OF ANGULAR VELOCITY AND SPEED

The mobile robot cannot move backward from the current position if it does not vary its attitude angle. Therefore, the robot needs to vary its attitude angle on the basis of its surrounding environment.

The mobile robot is required to reach the goal within a shorter period of time while avoiding collisions with walls and obstacles. The mobile robot needs to slow down to safely avoid obstacles present in a high-obstacle-density environment. In this section, we explain the method employed to control the angular velocity and speed of the robot.

4.1 Determination of angular velocity

It is important for mobile robot to perform sensing around the robot, especially in the direction of forward movement. Therefore, we utilize the difference in angle between 'the direction of forward movement' and 'the target angle', as shown in Fig. 9. The control strategy using the parameter is as follows: the higher its absolute value, the faster we make the robot vary its attitude angle as below.

$$\omega = k\Delta\theta (k > 0) \quad (6)$$

We vary the value of k depending on the minimum distance values obtained by ultrasonic sensors around the line. This distance value is denoted by l_p . The smaller the value of l_p , the larger the generated target angular velocity.

4.2 Determination of speed

In this subsection, we explain the method used to determine the target speed.

We determine the target acceleration for each sampling time T to consider the upper limit of the torque of the actuator. We generate a value in $[-1,1]$ and determine the target acceleration as the product of this value and the upper limit of the acceleration. We use the following data to determine the target acceleration.

- I_{mean} : mean of integration values
- l_p : distance around target angle
- $\Delta\theta_p$: temporal subtraction of θ_p
- $\Delta\theta$: difference between θ_p and forward direction
- $v(t-1)$: target speed one step ago

$\theta_p(t)$ and $v(t)$ respectively denote θ_p and v when the robot determines the t -th behavior. First, I_{mean} , l_p , $\Delta\theta_p$ and $\Delta\theta$ are converted into values in $[-1,1]$ using the functions f_1 , f_2 , f_3 and f_4 , respectively. However, f_2 is not a function of l_p but that of $2a_{\text{max}}l_p/v^2$. The physical meanings of the parameters $f_i (i=1\cdots 4)$ are as follows:

- f_1 : It is calculated by using integration value. It means density of obstacles around the robot.
- f_2 : It is calculated by information of traversable area. It means size of traversable area.
- f_3 : It is calculated by using time series data of target angle. Figuratively speaking, it means movement of the gaze.
- f_4 : It is calculated by using robot pose and target angle. It means largeness of input in order to move to the target angle.

Next, we represent the summation of the products of f_i and $r_i (i=1,2,3,4)$ as S as given below, provided that the summation of r_i is 1.

$$S = \sum_{i=1}^4 r_i f_i \quad \left(\sum_{i=1}^4 r_i = 1 \right) \tag{7}$$

If S is positive, we make the robot accelerate; otherwise, we make it slow down.

After this, we convert $v(t-1)$ into a value in $[0,1]$ using g , and the target acceleration is determined as the product of S , the upper limit of acceleration a_{max} and this value. However, we determine a threshold ε , and the target acceleration a is determined as 0 if $|S| < \varepsilon$.

Finally, the target speed $v(t)$ is determined as

$$v(t) = v(t-1) + a(t)T \tag{8}$$

Specifically, f_i is defined as below.

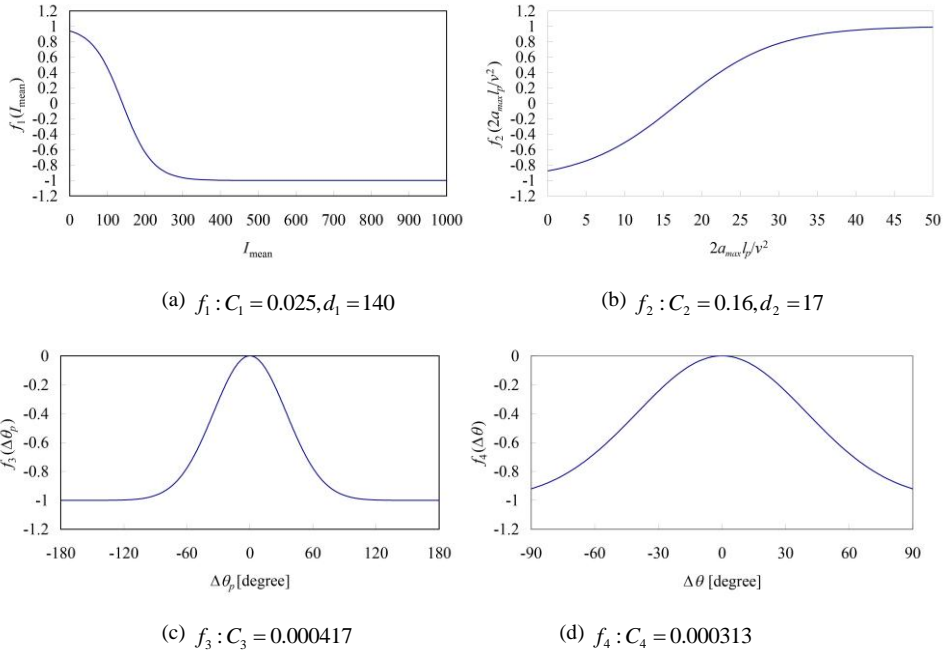


Fig. 10. Function $f_i (i = 1 \dots 4)$.

$$f_1(I_{mean}) = 1 - \frac{2}{1 + \exp\{-c_1(I_{mean} - d_1)\}}$$

$$f_2\left(\frac{2a_{max} l_p}{v^2}\right) = -1 + \frac{2}{1 + \exp\{-c_2(2a_{max} l_p / v^2 - d_2)\}}$$

$$f_3(\Delta\theta_p) = \exp\{-c_3(\Delta\theta_p)^2\}$$

$$f_4(\Delta\theta) = \exp\{-c_4(\Delta\theta)^2\}$$

Distributions of f_i are shown in Fig. 10. We defined $g(v)$ as given below.

$$g(v) = \begin{cases} \frac{v_{max} - v}{v_{max} - v_{min}} (S \geq 0) \\ \frac{v - v_{min}}{v_{max} - v_{min}} (S < 0) \end{cases} \quad (10)$$

An example of $g(v)$ is shown in Fig. 11.

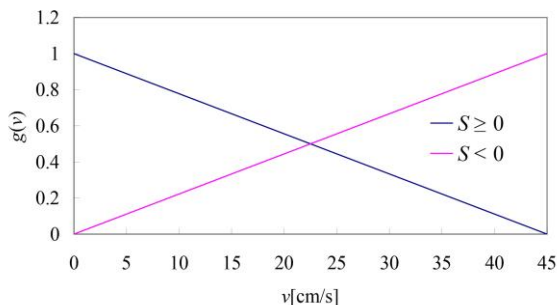


Fig. 11. $g(v)$ when v_{min} is 0cm/s and v_{max} is 45cm/s.

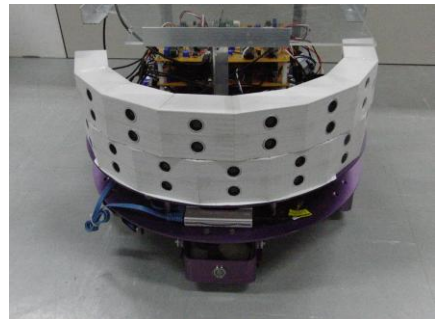


Fig. 12. Mobile robot mounted with sonar ring.

5. EXPERIMENTAL RESULTS

We conducted experiments using the omni-directional mobile robot equipped with the proposed sonar-ring system, as shown in Fig. 12. In this study, MDT-RO-02 from Mitsubishi Electric TOKKI System Co. was used as the omnidirectional mobile robot. The robot's specifications are: diameter = 390 mm, height = 151 mm, speed = 1.5 km/h (max), weight 8 kg, and payload = 15 kg (max). In these experiments, the robot determines its behaviour every 140 ms.

5.1 Speed control

To confirm the validity of the proposed method described in Section 4, we conducted experiments in several environments.

The values of f_i and r_i are shown in Tables 1 and 2, respectively. We determined the maximum and minimum values of the target speed as 0 and 45 cm/s, respectively, and the maximum value of the target acceleration as 55 cm/s².

At first, we show the results for the environment shown in Fig. 13 provided that the initial position of the robot is the origin and its initial forward direction is represented by the positive direction of the y -axis.

The trajectory of the robot is shown in Fig. 14. Dots represent position of the robot every 300 ms. Figures 15 and 16 show the variation in the target speed and acceleration with respect to time, respectively. The x -coordinate of the position of the robot exceeded 160 cm at 23.2 and 24.6 s. The robot accelerated until the y -coordinate of the position of the robot exceeded 330 cm, and then it turned toward the corner while slowing down. Right side of Fig. 14 shows the trajectory when the target speed is fixed at 30 cm/s. The x -coordinate of the position of the robot exceeded 160 cm at 19.1 s.

Even with a constant target speed, the robot could safely avoid collisions with walls and moved more rapidly when compared to the case in which the proposed method was applied in this environment. The reason for this is that the robot could not accelerate sufficiently when it moved linearly. In the proposed method, the maximum value of S is considerably smaller than 1 because the maximum value of f_3 and f_4 is 0. Thus, the robot cannot accelerate sufficiently when it follows a straight path, where there are few obstacles.

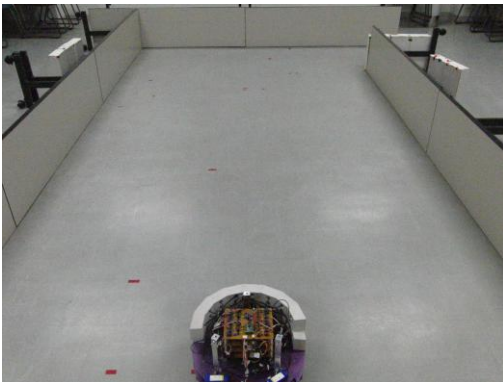


Fig. 13. Experimental environment 2.

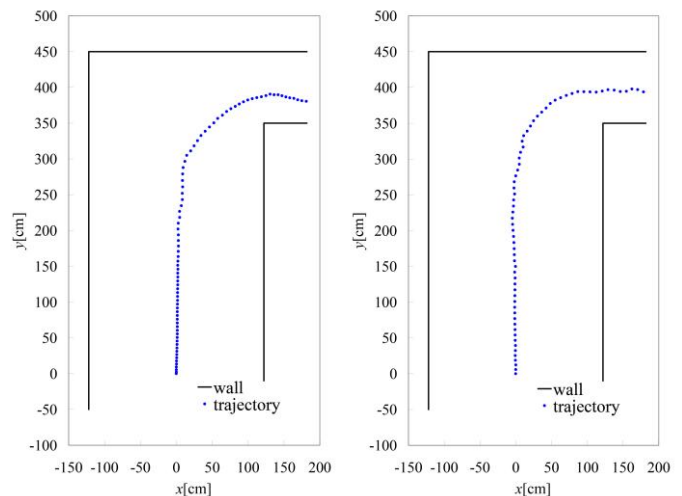


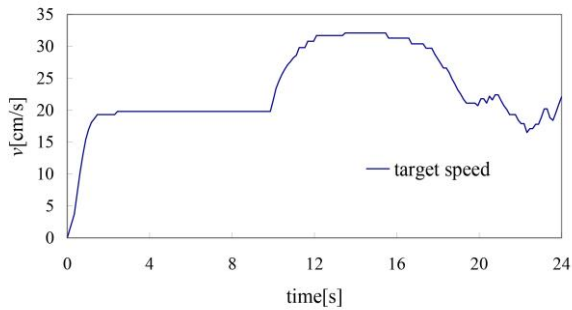
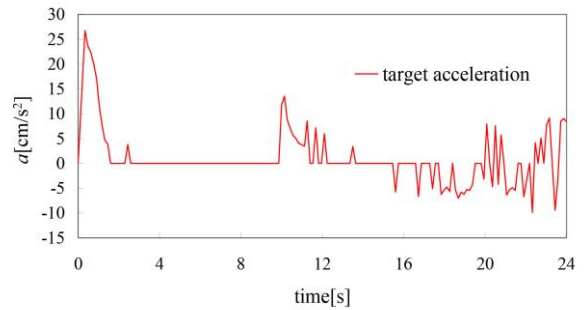
Fig. 14. Left shows the trajectory in environment 2. Right is obtained constant speed: $v = 30$ cm/s.

Table 1: Parameters of f_i

c_1	0.025
d_1	140
c_2	0.16
d_2	17
c_3	0.000417
c_4	0.000313

Table 2: Parameters of r_i

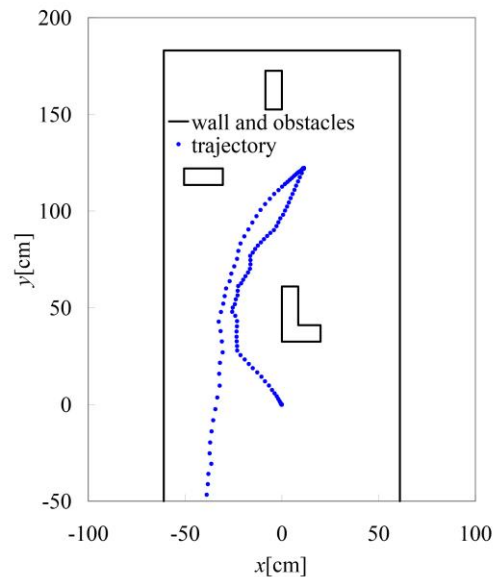
r_1	0.22
r_2	0.32
r_3	0.24
r_4	0.22

**Fig. 15.** Temporal variability in target speed in environment 2.**Fig. 16.** Temporal variability in target acceleration in environment 2.

5.2 Deadlock avoidance

We conducted experiments in the environment shown in Fig. 17 by applying the proposed method for the detection of deadlocks. The values of w_1 , w_2 , w_3 and c were 0.0135, 0.00634, -0.570 , and 1.00, respectively, and the robot determined that no passable area exists in the sensing range when the value of ζ is greater than 0.97.

The trajectory is shown in Fig. 18. The robot detected a dead end and rotated by 180 degrees around the point (11,122). The variation in ζ with respect to time before it becomes larger than 0.97 is shown in Fig. 19.

**Fig. 17.** Experimental environment 3.**Fig. 18.** Trajectory of robot in environment 3.

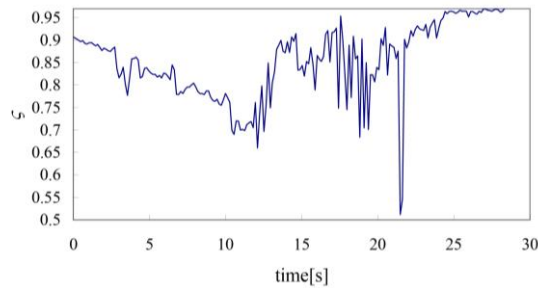


Fig. 19. Temporal variability in ζ .

6. CONCLUSIONS

This paper proposes a novel sonar-ring system, which utilizes an integration-type ultrasonic wave sensor. In this study, using this integration-type sonar-ring system, we devised a method for determining the local behavior of a robot. The experimental results show that with the proposed system, an omnidirectional mobile robot develops the ability to generate an appropriate path to avoid collisions with obstacles.

The results also showed that the robot determined the target speed on the basis of the environment. The speed of the robot especially decreased in an environment with many obstacles. However, the robot could not accelerate sufficiently in wide passage with few obstacles. Therefore, we need to improve the proposed method to make the robot accelerate more when it goes straight in wide corridor environment. Future study will focus on improving the proposed method for enabling the robot to accelerate further when moving straight in a wide corridor with few obstacles.

7. ACKNOWLEDGEMENT

This work was supported by JSPS KAKENHI Grant Number 26420408.

REFERENCES

- [1] Borenstein, J. and Koren, Y. Histogramic In-Motion mapping for mobile robot obstacle avoidance, *IEEE Transactions on Robotics and Automation*, Vol. 7(4), 1991, pp. 535-539.
- [2] Borenstein, J. and Koren, Y. Error eliminating rapid ultrasonic firing for mobile robot obstacle avoidance, *IEEE Transactions on Robotics and Automation*, Vol. 11(1), 1995, pp. 132-138.
- [3] Wehn, H.W. and Belanger, P.R. Ultrasound-Based robot position estimation, *IEEE Transactions on Robotics and Automation*, Vol. 13(5), 1997, pp. 682-692.
- [4] Nakamura, T., Takamura, S. and Asada, M. Behavior-Based map representation for a sonar-based mobile robot by statistical methods, *IEEE/RSJ Int. Conf. Intelligent Robots and Systems*, Vol. 1, 1986, pp. 276-283.
- [5] Mataric, M.J. Integration of representation into goal-driven behavior-based robots, *IEEE Transactions on Robotics and Automation*, Vol. 8(3), 1992, pp. 304-312.
- [6] Cahut, L., Valavanis, K.P. and Delic, H. Sonar resolution-based environment mapping, *IEEE International Conference on Robotics and Automation*, Vol. 3, 1998, pp. 2541-2547.
- [7] Emaru, T., Kazuo, T. and Tsuchiya, T. Speed control of a sonar-based mobile robot with considering the self-localization, *IEEE Int. Conference on Mechatronics and Automation*, Vol. 1, 2005, pp. 125-130.
- [8] Emaru, T. and Tsuchiya, T. Implementation of unconsciousness movements for mobile robot by using sonar sensor, *International Conference on Control, Automation and Systems*, 2007, pp. 17-20.
- [9] Emaru, T., Hoshino, Y and Kobayashi, Y. Speed control of a sonar-based mobile robot by considering the limitation of accelerated velocity, *Journal of System Design and Dynamics*, Vol. 4(1), 2010, pp. 38-49.
- [10] Mur-Artal, R., Montiel, J.M.M. and Tardos, J.D. ORB-SLAM: A versatile and accurate monocular SLAM system, *IEEE Transactions on Robotics*, Vol. 31(5), 2015, pp. 1147-1163.
- [11] Macdonald, J., Leishman, R., Beard, R. et al. Analysis of an improved IMU-based observer for multirotor helicopters, *Journal of Intelligent & Robotic Systems*, Vol. 74(3), 2014, pp. 1049-1061.
- [12] Whelan, T., Kaess, M., Johannsson, H., Leonard, J.J. et al. Real-time large-scale dense RGB-D SLAM with volumetric fusion, *The International Journal of Robotics Research*, Vol. 34(4-5), 2015, pp. 598-626.